Short communication

3D-printable CFR polymer composites with dual-cure sequential IPNs

Gianmarco Griffini, Marta Invernizzi, Marinella Levi, Gabriele Natale, Giovanni Postiglione, Stefano Turri*

Department of Chemistry, Materials and Chemical Engineering "Giulio Natta", Politecnico di Milano, Piazza Leonardo da Vinci 32, 20133 Milan, Italy

A B S T R A C T

In this work a sequential interpenetrating polymer network (IPN) obtained by co-formulation of a photocurable acrylic resin with a thermocurable epoxy resin is presented and proposed as matrix for the fabrication of carbon-fiber reinforced (CFR) composite structures by means of 3D-printing technology. This approach combines the advantages of the easy free-form fabrication typical of the 3D-printing technology with the purposely customized features of the newly developed IPN material. Photo-calorimetric and dynamic-mechanical analyses were performed in order to investigate the photo- and thermal-crosslinking reactions and their effect on the development of the IPN system. The IPN resin was finally loaded with carbon fibers and successfully ultraviolet-assisted (UV)-3D printed, demonstrating the possibility of fabricating CFR composite materials in 3D with excellent mechanical properties. Being the first example of direct fabrication of IPN-based composites by 3D printing, this study clearly shows the great potential of this additive manufacturing technology for advanced industrial applications.

1. Introduction

The interest in 3D printing from the manufacturing industry has risen considerably in the last few years due to the many appealing features of this technology, such as its ability to realize complex geometries, the ease of personalization of the manufactured product, and the potential logistical advantages offered by the diffuse manufacturing paradigm. As a consequence, the demand for tailored 3D-printable materials with improved structural and functional properties is continuously growing, with polymers still playing a dominant role [1–5].

In many fields, 3D-printing by fused deposition modeling (FDM) is widely used as rapid prototyping technology, in which thermoplastic polymer filaments (ABS, PLA, and a few others) are employed as structural inks. In order to shift away from the mere production of prototypes, more performing materials, especially in terms of mechanical and thermal properties, are required. Some attempts were made to reinforce thermoplastics with fillers, short fibers or post processing techniques. Despite some observed increase in materials performance, these strategies still rely on the FDM technology [6,7] and on the consequent need to process pre-extruded filaments.

Received 6 November 2015
Accepted 15 March 2016
Available online 17 March 2016

Along with FDM technology, ultraviolet-assisted 3D (UV-3D) printing has been more recently proposed and developed for the fabrication of a variety of 3D microstructures with peculiar properties [8,9]. This technology consists in the additive deposition of layers of a photocurable liquid polymer, which is crosslinked by an external UV light source as soon as it flows out of the nozzle during the printing process. The photocurable liquid precursor can be easily modified by formulation according to the desired final material properties. To this end, the use of embedded nano- and micro-particles has been demonstrated, leading to the production of reinforced components, conductive microstructures and microcoils [8–11]. However, this technology has not yet been exploited for the fabrication of fiber-reinforced composites to date. This is partially due to the fact that UV-3D printing strictly requires materials with fast curing kinetics and loading with non-transparent particles or fibers may influence the UV light transmission through the sample, causing the inhibition of the polymerization or drastically slowing down its rate [12,13]. Moreover, UV curable resins often do not offer sufficiently high mechanical properties to be used for the fabrication of high performance fiber-reinforced composites.

In the light of the above considerations, the development of engineered polymeric systems capable to form sequential interpenetrating polymer networks (IPN) by dual-cure mechanisms can offer significant advantages for this application. Specific

* Corresponding author.
E-mail address: stefano.turri@polimi.it (S. Turri).

Published Journal Article available at: http://dx.doi.org/10.1016/j.polymer.2016.03.048

mechanical properties can be achieved when multifunctional polymers are entangled at the nanometric scale as in IPNs. Indeed, their peculiar chemical structure and morphology has favored their widespread diffusion in a variety of applications [14–19].

In this communication, we report on an easily 3D-printable carbon fiber reinforced (CFR) polymer composite formulation based on a new photo-thermocurable IPN system. The material is successfully processed to form stable 3D structures by using a low cost, home-modified UV-3DP apparatus. A subsequent thermal treatment of the UV-3D printed object is performed to complete the crosslinking process and achieve full mechanical properties. Dual-cure resins have already been used for rapid prototyping, including the manufacturing of carbon fiber materials *via* photolithography [20] and stereolithography [21]. However, to the best of our knowledge, this is the first report on the direct UV-3D printing of CFR polymer composites with an IPN-based dual-cure ink.

2. Experimental

2.1. Raw materials

Bisphenol A diglycidyl ether (DGEBA), 1,1-dimethyl, 3-(3′,4'-dichlorophenyl) urea (Diuron™), dicyandiamide (DICY), and fumed silica (200 m^2/g, primary particle size distribution 8–20 nm, OX200 throughout the manuscript) were purchased from Sigma–Aldrich and used as received. Bisphenol A ethoxylate diacrylate (SR349) was kindly provided by Arkema, whilst the photoinitiator 2,4,6-trimethylbenzoylphenyl phosphinate (Irgacure TPO-L, TPO-L throughout the manuscript) was obtained from BASF. Carbon fibers were kindly provided by Zoltek (Panex™ 30 milled Carbon Fibers, 99% carbon, density 1.8 g/mL, fiber diameter 7.2 μm, fiber length 100–150 μm).

2.2. Resin and composite formulation and curing

Formulations were obtained by liquid blending the photocurable acrylic resin and the thermocurable epoxy resin with suspended hardener (DICY) and accelerator (Diuron™). The photocurable acrylic resin was a stock solution of SR349 doped with 3 wt% TPO-L mixed under magnetic stirring at room temperature for 30 min (indicated as p-A resin in the following). For the epoxy resin formulation (t-E resin in the following), 20 g of liquid DGEBA, 1.36 g (6.19% w/w) of DICY and 0.66 g (3% w/w) of Diuron™ were poured into a beaker, stirred at 100 °C for 1 h and then mixed with an ultrasonicator tip (Sonic & Materials VCX130, power 130 W, frequency 20 kHz) to form a finely dispersed suspension. The epoxy system behaves as a monocomponent since no reaction occurs until the unsoluble DICY remains phase separated (that is for T < 150 °C). The final dual-cure formulation was obtained by mixing the p-A resin and the t-E resin under magnetic stirring at 70 °C for 30 min at a 1:1 weight ratio (M50 sample). Characterizations concerning IPN systems were mostly performed on M50 formulation.

For 3D printing tests, four other formulations were developed with increasing weight concentrations of p-A component, namely 5%, 10%, 15% and 20% by weight (indicated as M5, M10, M15, M20 in the following). Since the two starting resins and their blends are essentially low viscosity Newtonian liquids, depositing them from the syringe dispenser of the 3D printer resulted into a significant lateral spreading with poor control of 3D geometries. In order to solve this issue, a fixed amount of fumed silica (7% w/w) as thixotropic additive was added to all the formulations, making them suitable for 3D printing. The CFR composites for 3D printing were based on M50 formulation and were obtained by adding 5% and 30% w/w of carbon fibers (CF5 and CF30 samples, respectively).

The thermal curing cycle after 3D-printing was carried out at 220 °C for 20 min in a ventilated oven.

2.3. Characterization techniques

The thermal characterization of the IPN system and its precursors was performed using a differential scanning calorimeter (DSC). DSC scans were carried out on a Mettler–Toledo DSC/823^e instrument, indium and n-hexane calibrated, heating from 20 °C to 250 °C with a rate of 20 °C/min in N_2 environment. Photocalorimetric tests were carried out at ambient temperature on 10–50 mg samples by coupling the DSC instrument with a UVA light source (Lightningcure LC8 by Hamamatsu, 98 mW/cm^2, 300–450 nm wavelength range) under N_2 atmosphere. The heat of reaction was obtained by integration of the resulting exotherms.

Dynamic mechanical analyses (DMA) in three-point bending mode were carried out on a Mettler Toledo DMA/SDTA861 instrument at ambient temperature in strain sweep, and in dynamic scans from 20 °C to 250 °C at a heating rate of 3 °C/min. The frequency was kept constant at 1 Hz.

Scanning electron microscopy (SEM) was performed on fractured M50 surfaces with a Carl Zeiss EVO 50 Extended Pressure scanning electron microscope (acceleration voltage of 15.00–17.50 kV) to evaluate the IPN morphology. Samples were subjected to an alkaline etching (10% KOH in methanol for 1 h at 60 °C) to selectively remove or damage the acrylic phase.

2.4. 3D-printing experiments

A low-cost, home-assembled 3Drag 1.2 benchtop printer (Futura Elettronica, Italy) incorporating a syringe dispenser equipped with two 3W UV-A torches (WF-501B by Ultrafire Ltd, China) with light emission peaked at 405 nm was used for UV-3D printing the IPN composites (M5-M50, CF5, CF30). Print speed ranged between 1 and 10 mm/s and a 0.84 mm nozzle diameter was used. An image of the set-up used is shown in Fig. 1. The image of the 3D-object to be fabricated is shown in Fig. 2a. It was designed using “Solidworks” software (Dassault Systèmes, France) to test the ability to print cantilevered geometries with different inclinations. In order to process the 3D model, the open source slicing software “Cura” (Ultimaker B.V., Holland) was used, and the printing test was carried out using spiral slicing option and a single wall thickness.

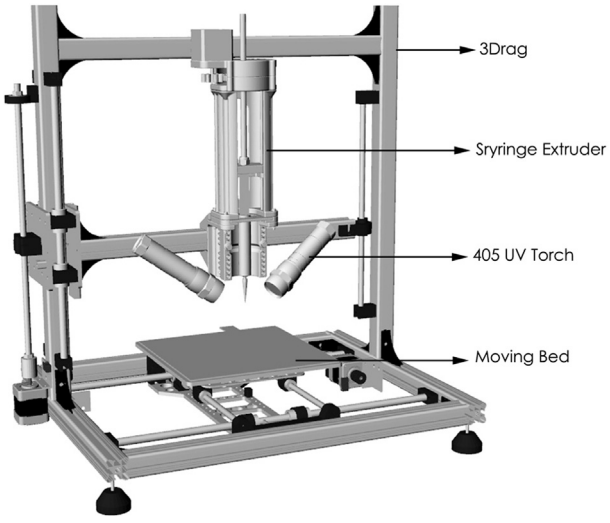

Fig. 1. Schematic representation of the UV-3D printing equipment employed in this work.

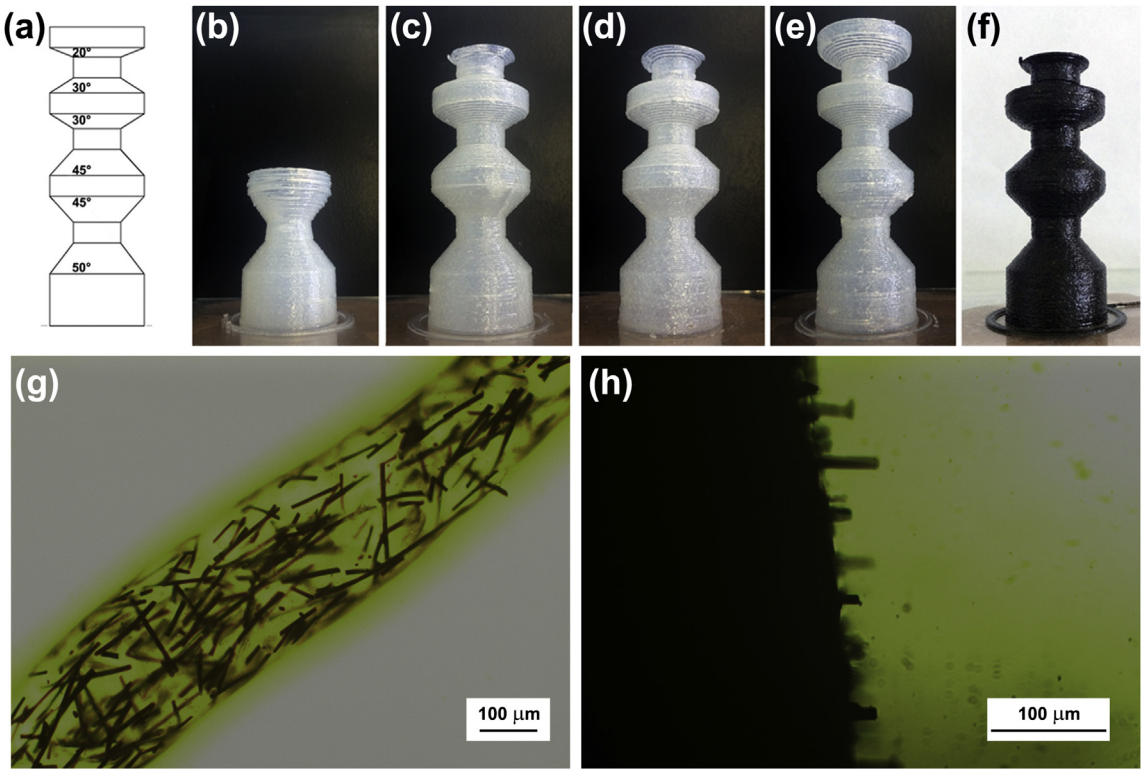

Fig. 2. (a) layout of the target 3D model used to assess the printability of the inks developed in this work; UV-3D printed reproduction of the target model using (b) M5, (c) M10, (d) M15, (e) M20, and (f) CF5; optical microscopy image of (g) CF5 liquid filament and (h) cryo-fractured UV-3D printed CF5 surface.

3. Results and discussion

The 3D-printing processability of the acrylic-epoxy IPN formulations and corresponding composites was assessed. All the formulations from M5 to M50 were loaded into the syringe, and printed in the attempt to reproduce the target 3D model whose frontal projection is presented in Fig. 2a. Such 3D model is constituted by a vertical column with overhanging features with angles ranging from 50° at the bottom to 20° at the top. The smaller the inclination angle the more challenging it is to print the material *via* layer-by-layer deposition without incurring into resin sagging or spreading. Therefore, this 3D model represents a convenient test designed to verify the ink processability while printing complex parts. During the printing process, it was found that all formulations were able to flow out of the nozzle and harden upon exposure to the UV sources embedded into the 3D printer (Fig. 1). The results of the printing tests on samples M5-M20 and CF5 are presented in Fig. 2b–e. The sample M5, containing only 5% w/w of photocurable p-A resin, remained too soft after the photocuring process. Therefore, this ink did not allow to obtain a complete UV-3D print of the 3D target model, as already the first 45° overhang was found to show some visible structural imperfections (Fig. 2b). By increasing the p-A concentration to 10% w/w (M10, Fig. 2c) and 15% w/w (M15, Fig. 2d) the printing quality was found to improve considerably as the material showed a solid-like behavior after UV exposure. The UV-3D printed model objects obtained with these formulations were very similar and only showed some visible structural defects during the top 20° overhang which could thus not be completely printed. On the other hand, the M20 ink allowed for a successful 3D printed reproduction of the target 3D model (Fig. 2e), thus demonstrating that a 1:5 weight ratio between p-A and t-E constitutes the minimum photopolymer concentration needed to reach optimal printing performance even in the presence of steeply overhanging parts. When considering carbon-fiber reinforced (CFR) composites, it was found that a higher fraction of photocurable resin was needed for correct ink processing, likely due to the presence of the black carbon fibers that are responsible for a lower photopolymerization efficiency. For this reason, all the experiments with CFR composites were performed based on M50 as resin matrix. As shown in Fig. 2f, UV-3D printing of CFR composites based on CF5 formulation could be successfully demonstrated up to an overhang of 30°.

Optical microscopy analysis on the deposited CF5 liquid filament (before curing) showed that a portion of the carbon fibers embedded in the polymeric matrix maintains their structural integrity upon 3D printing without breaking apart, in addition to appearing partially oriented in the direction of the extrusion (Fig. 2g). This observation is also confirmed by optical microscopy image of the fractured surface that shows clear alignment of the carbon fibers in the proximity of the fracture (Fig. 2h). In the case of CF30 material, the viscosity was found to be too high to allow for an easy 3D deposition from the printer nozzle, and only simpler flat specimens suitable for further mechanical testing were realized. Furthermore, printed specimens from this ink only showed a semi-solid behavior immediately after printing, calling for the need of a subsequent exposure to UV-A to dry them completely before the final thermal treatment.

The photocuring process and the photopolymerization conversions were investigated by photocalorimetric measurements, and the results are shown in Fig. 3a–d. The enthalpy of polymerization of CF5 system was found to be about 111 J/g (Fig. 3b), which accounts for 92.5% of the enthalpy of polymerization reported for the unfilled M50 resin (Fig. 3a). This difference could be likely attributed to the presence of carbon fibers in the CF5 system that may partially prevent full access of the UV radiation to the photocurable resin, thus lowering the total heat of reaction. The same CF5

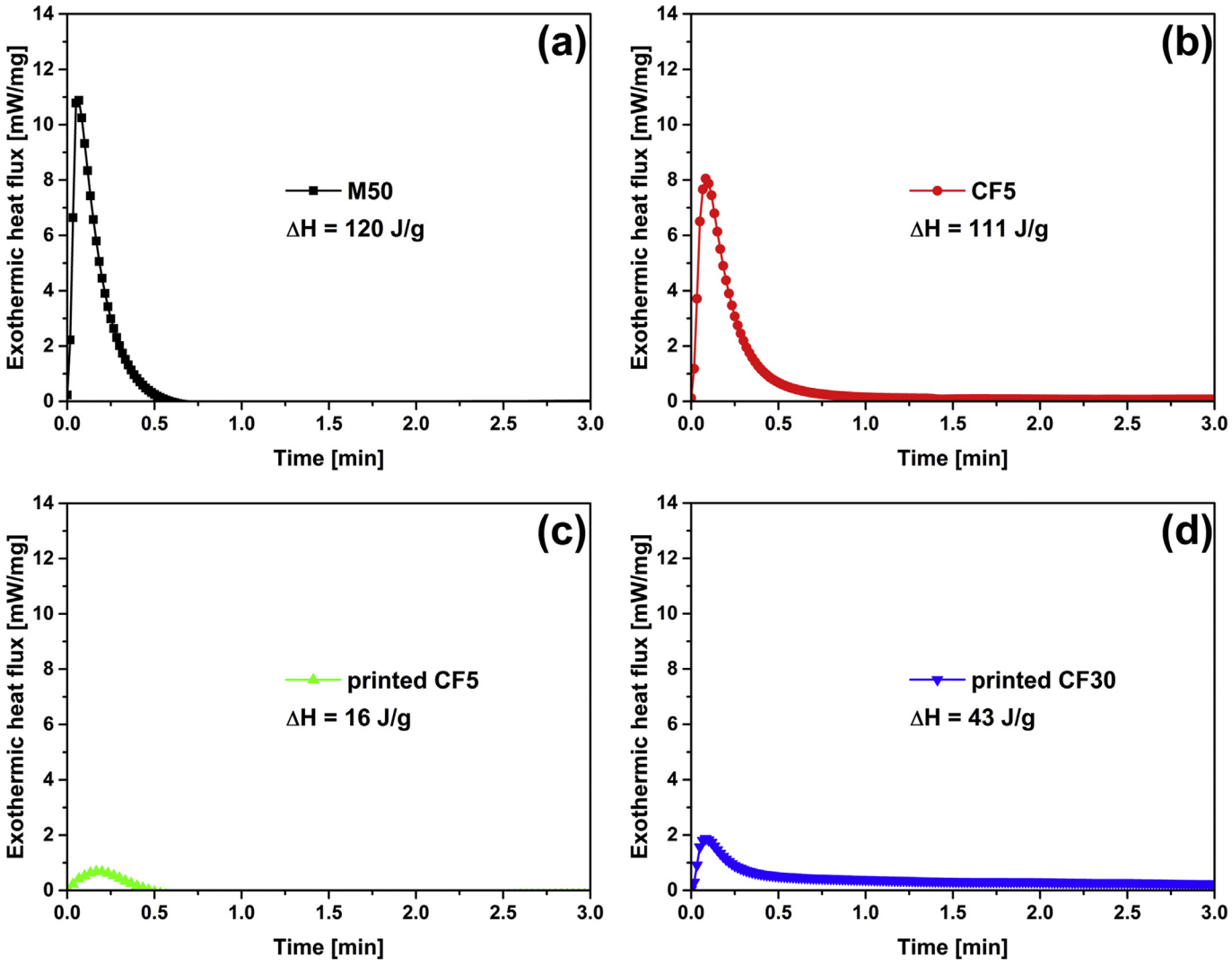

Fig. 3. Photocalorimetric (photo-DSC) scans of (a) M50 formulation before printing, (b) CF5 formulation before printing, (c) printed CF5 formulation, and (d) printed CF30 formulation.

material after the 3D-printing cycle showed a residual enthalpy of 16 J/g (Fig. 3c), that corresponds to an apparent photocuring conversion after the UV-3D printing process of about 85%. The photocuring conversion after UV-3D printing found for the 30CF composite system was significantly lower (51% after normalization by the effective fraction of UV-curable component). This behavior can be very likely ascribed to a strong UV-absorbing action of the highly concentrated carbon fibers present in this formulation.

In order to investigate the morphology of the obtained dual-cure resins and 3D printed parts, SEM images were taken on the M50 sample after fracture and subsequent exposure to a 10% w/w solution of KOH in methanol for 1 h at 60 °C to selectively etch the acrylic phase (Fig. 4). Clearly, a highly interconnected IPN structure is formed upon full dual-curing with typical sizes ranging from 10^1 to 10^2 nm.

The mechanical behavior and thermal transitions of the developed dual-cure inks were preliminarily investigated by means of DMA and DSC analyses. Results are summarized in Table 1, where the experimental values for the storage modulus E′ at room temperature and the temperature at the tanδ peak as obtained from DMA as well as the glass transition temperature (Tg) as measured *via* DSC are presented.

As it appears from Table 1, a significant increase of both Tg (from 73 °C to 115 °C) and storage modulus (from 2.5 GPa to 3.0 GPa) can be obtained by re-formulating the UV curable resin in the form of an IPN dual-cure system. In addition, one single Tg was observed in the IPN system, as a further demonstration of the excellent structural homogeneity of the materials [18]. High storage moduli were measured also for the CFR composites (3.8 GPa and 7.7 GPa for the CF5 and CF30 composite formulations, respectively). The measured data were compared with those predicted by the Halpin-Tsai model for random, discontinuous fiber reinforced composites [22].

$$E = E_m \frac{1 + \eta\zeta v_f}{1 - \eta v_f} \tag{1}$$

$$\eta = \frac{E_f / E_m - 1}{E_f / E_m + \zeta} \tag{2}$$

with E, E_m, ζ, v_f and E_f being the modulus of the composite material, the modulus of the matrix, the fiber aspect ratio, the volume fraction of the fibers and the modulus of the fiber, respectively.

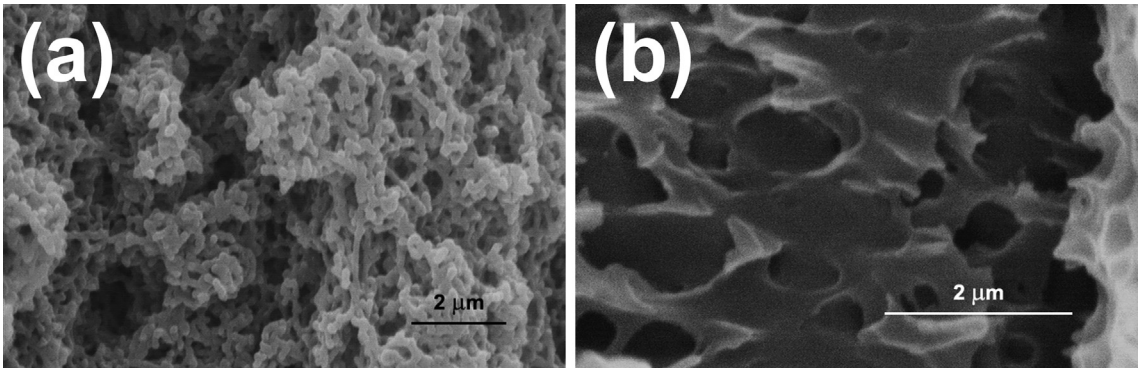

Fig. 4. SEM images of fractured surface of UV-3D printed M50 samples after alkaline etching.

Table 1
Storage modulus E′ and temperature at the tanδ peak as obtained from DMA, and Tg value obtained from DSC measurements of crosslinked resins and CFR composites.

	p-A resin	M50	CF5	CF30
E' (25 °C, GPa)	2.5 ± 0.2	3.0 ± 0.4	3.8 ± 0.2	7.7 ± 0.2
Max tanδ (°C)	73	115	139	76
Tg_{DSC} (°C)	37	103	n.d.	n.d.

Eq. (1) was fitted using the storage modulus of the carbon fibers $E_f = 200$ GPa and $\zeta = 2\ l/d = 13.8$, where l and d are the length and the diameter of the reinforcing fiber, respectively. Measured moduli for composites were found to be systematically lower than the limiting theoretical values obtained from the Halpin–Tsai model. In particular, a theoretical value of storage modulus of 5.6 GPa was calculated for the CF5 composite systems, as opposed to a measured value of 3.8 GPa. Larger differences were observed for the CF30 system that showed a theoretically predicted storage modulus of 19.8 GPa compared to an experimentally measured value of 7.7 GPa. A possible explanation for such discrepancies may lie in the likely and unavoidable overestimation of fiber aspect ratio l/d in the actual samples (some fibers are clearly broken during the printing process as shown in Fig. 2). In addition, in the case of the CF30 composite system, the unusually low value of Tg measured for this material may also play a role as this may be related to non-complete crosslinking and thus lower storage modulus. Nevertheless, the values found experimentally on the systems investigated in this work are in good agreement with experimental results reported in the literature on composites systems with the same type of reinforcing fibers [23,24,25].

4. Conclusion

In conclusion, a new dual-cure IPN system was presented in this work obtained by blending a photocurable acrylic resin and a thermally reactive epoxy resin. The very fast UV-curing kinetics of the photocurable resin makes the IPN system very suitable for a rapid UV-assisted 3D printing, whilst the following thermal curing of the epoxy component confers enhanced thermo-mechanical properties to the printed part. The 3D-printing tests suggested that the weight ratio between the photocurable and the thermally curable components in the IPN system strongly influences the behavior of the dual-cure ink upon printing in such a way that its fine-tuned control is essential to achieve desirable final printing features. For the first time, UV-assisted 3D printing was also employed to successfully process CFR polymer composites based on an optimized dual-cure formulation. The concentration of carbon fibers in the composite ink was found to significantly affect the efficiency of the UV-curing process, thus indicating that successful UV-3D printing of high-fiber-content composites needs sufficiently high power UV sources to be accomplished. The results of this study open the way towards the digital fabrication of high performance composite materials through 3D printing technology.

References

[1] B.Y. Ahn, S.B. Walker, S.C. Slimmer, A. Russo, A. Gupta, S. Kranz, E.B. Duoss, T.F. Malkowski, J.A. Lewis, Planar and three-dimensional printing of conductive inks, J. Vis. Exp. 58 (2011) 3189, http://dx.doi.org/10.3791/3189.
[2] S.J. Leigh, R.J. Bradley, C.P. Purssell, D.R. Billson, D.A. Hutchins, A simple, low-cost conductive composite material for 3D printing of electronic sensors, Plos One 7 (2012) 11, http://dx.doi.org/10.1371/journal.pone.0049365.
[3] S.J. Leigh, R.J. Bradley, C.P. Purssell, D.R. Billson, D.A. Hutchins, Using a magnetite/thermoplastic composite in 3D printing of direct replacements for commercially available flow sensors, Smart Mater. Struct. 23 (2014) 095039, http://dx.doi.org/10.1088/0964-1726/23/9/095039.
[4] A. Ian, I.A. Barker, M.P. Ablett, H.T.J. Gilbert, S.J. Leigh, J.A. Covington, J.A. Hoyland, S.M. Richardson, A.P. Dove, A microstereolithography resin based on thiol-ene chemistry: towards biocompatible 3D extracellular constructs for tissue engineering, Biomater. Sci. 2 (2014) 472, http://dx.doi.org/10.1039/c3bm60290g.
[5] G. Postiglione, G. Natale, G. Griffini, M. Levi, S. Turri, Conductive 3D microstructures by direct 3D printing of polymer/carbon nanotube nanocomposites via liquid deposition modeling, Compos. A 76 (2015) 110, http://dx.doi.org/10.1016/j.compositesa.2015.05.014.
[6] J.T. Belter, A.M. Dollar, Strengthening of 3D printed fused deposition manufactured parts using the fill compositing technique, Plos One 10 (2015) 4, http://dx.doi.org/10.1371/journal.pone.0122915.
[7] F. Ning, W. Cong, J. Qiu, J. Wei, S. Wang, Additive manufacturing of carbon fiber reinforced thermoplastic composites using fused deposition modeling, Compos. B 80 (2015) 369, http://dx.doi.org/10.1016/j.compositesb.2015.06.013.
[8] L.L. Lebel, B. Aissa, M.A. El Khakani, D. Therriault, Ultraviolet-assisted direct-write fabrication of carbon nanotube/polymer nanocomposite microcoils, Adv. Mater. 22 (2010) 592, http://dx.doi.org/10.1002/adma.200902192.
[9] G. Postiglione, G. Natale, G. Griffini, M. Levi, S. Turri, UV-assisted three-dimensional printing of polymer nanocomposites based on inorganic fillers, Polym. Compos. (2015), http://dx.doi.org/10.1002/pc.23735.
[10] R.D. Farahani, H. Dalir, V. Le Borgne, L.A. Gautier, M.A. El Khakani, M. Lévesque, D. Therriault, Direct-write fabrication of freestanding nanocomposite strain sensors, Nanotechnol. 23 (2012) 085502, http://dx.doi.org/10.1088/0957-4484/23/8/085502.
[11] R.D. Farahani, L.L. Lebel, D. Therriault, Processing parameters investigation for the fabrication of self-supported and freeform polymeric microstructures using ultraviolet-assisted three-dimensional printing, J. Micromech. Microeng. 24 (2014) 055020, http://dx.doi.org/10.1088/0960-1317/24/5/055020.
[12] A. Endruweit, M.S. Johnson, A.C. Long, Curing of composite components by ultraviolet radiation: a review, Polym. Compos. 27 (2006) 119, http://dx.doi.org/10.1002/pc.20166.
[13] A. Endruweit, W. Ruijter, M.S. Johnson, A.C. Long, Transmission of ultraviolet light through reinforcement fabrics and its effect on ultraviolet curing of composite laminates, Polym. Compos. 29 (2008) 818, http://dx.doi.org/10.1002/pc.20483.
[14] L.H. Sperling, Interpenetrating polymer networks: an overview, Adv. Chem. 239 (1994) 3, http://dx.doi.org/10.1021/ba-1994-0239.ch001.
[15] L.H. Sperling, V. Mishra, The current status of interpenetrating polymer networks, Polym. Adv. Technol. 7 (1996) 197, http://dx.doi.org/10.1002/(SICI)1099-1581(199604)7:4<197::AID-PAT514>3.0.CO;2–4.
[16] L.K. Kostanski, R. Huang, C.D.M. Filipe, R. Ghosh, Interpenetrating polymer

networks as a route to tunable multi-responsive biomaterials: development of novel concepts, J. Biomater. Sci. 20 (2009) 271, http://dx.doi.org/10.1163/156856208X3999107.
[17] S. Simic, B. Dunjic, S. Tasic, B. Bozic, D. Jovanovic, I. Popovic, Synthesis and characterization of interpenetrated polymer networks with hyperbranched polymers through thermal-UV dual curing, Prog. Org. Coat. 63 (2008) 43, http://dx.doi.org/10.1016/j.porgcoat.2008.04.006.
[18] S. Marinovic, I. Popovic, B. Dunjic, S. Tasic, B. Bozic, D. Jovanovic, The influence of different components on interpenetrating polymer network's (IPNs) characteristics as automotive top coats, Prog. Org. Coat. 68 (2010) 293, http://dx.doi.org/10.1016/j.porgcoat.2010.03.010.
[19] M. Sangermano, W. Carbonaro, G. Malucelli, A. Priola, UV-cured interpenetrating acrylic-epoxy polymer networks: preparation and characterization, Macromol. Mat. Eng. 293 (2008) 515, http://dx.doi.org/10.1002/mame.200800020.
[20] A. Gupta, A.A. Ogle, Dual curing of carbon fiber reinforced photoresins for rapid prototyping, Polym. Compos. 23 (2002) 1162–1170, http://dx.doi.org/10.1002/pc.10509.
[21] P.J. Bartolo, G. Mitchell, Stereo-thermal-lithography: a new principle for rapid prototyping, Rapid Prototyp. J. 9 (2003) 150, http://dx.doi.org/10.1108/13552540310477454.
[22] J.C. Halpin, J.L. Kardos, The Halpin–Tsai equations: a review, Polym. Eng. Sci. 16 (1976) 344, http://dx.doi.org/10.1002/pen.760160512.
[23] P. Tsotra, K. Friedrich, Electrical and mechanical properties of functionally graded epoxy-resin/carbon fibre composites, Compos. A 34 (2003) 75, http://dx.doi.org/10.1016/S1359-835X(02)00181-1.
[24] H. Zhang, Z. Zhang, C. Breidt, Comparison of short carbon fibre surface treatments on epoxy composites I. Enhancement of the mechanical properties, Compos. Sci. Technol. 64 (2004) 2021, http://dx.doi.org/10.1016/j.compscitech.2004.02.009.
[25] B.G. Compton, J.A. Lewis, 3D-printing of lightweight cellular composites, Adv. Mater. 26 (2014) 5930, http://dx.doi.org/10.1002/adma.201401804.